Mass dependence of the heavy quark potential and its effects on quarkonium states

Alexander Laschka, Norbert Kaiser, and Wolfram Weise
Physik Department
Technische Universität München
D-85747 Garching, GERMANY

The heavy quark-antiquark potential is accessible in perturbative QCD and in lattice simulations. The perturbative short-distance part of the potential is contructed via a restricted Fourier transform, covering the momentum region where perturbative QCD is applicable. We show that for the leading order static term as well as for the mass dependent corrections, the perturbative part can be matched at intermediate distances with results from lattice QCD. From these matched potentials, quarkonium spectra with a single free parameter (the heavy quark mass) are derived and compared with empirical spectra. Furthermore, charm and bottom quark masses are deduced.

1 The static potential

The potential between two heavy quarks is a prime subject of interest since the early days of QCD. Nowadays it is defined in a non-relativistic effective theory framework. While the long distance part can be studied in lattice QCD simulations, perturbation theory should be expected to work at short distances. The potential can be organized in a power series of the inverse quark mass m:

$$V = V^{(0)} + \frac{V^{(1)}}{m/2} + \frac{V^{(2)}}{(m/2)^2} + \dots . \tag{1}$$

The leading term $V^{(0)}$ represents the static potential. It has the following form at two-loop order in momentum space:

$$\tilde{V}^{(0)}(|\vec{q}\,|) = -\frac{16\pi\alpha_s(|\vec{q}\,|)}{3\vec{q}^{\,2}} \left\{ 1 + \frac{\alpha_s(|\vec{q}\,|)}{4\pi}\, a_1 + \left(\frac{\alpha_s(|\vec{q}\,|)}{4\pi}\right)^2 a_2 + \dots \right\}, \tag{2}$$

where $\vec{q}$ is the three-momentum transfer. The constants a_1 and a_2 are [1–3]:

$$a_1 = 31/3 - 10/9\, n_f, \tag{3}$$

$$a_2 = 456.749 - 66.3542\, n_f + 1.23457\, n_f^2, \tag{4}$$

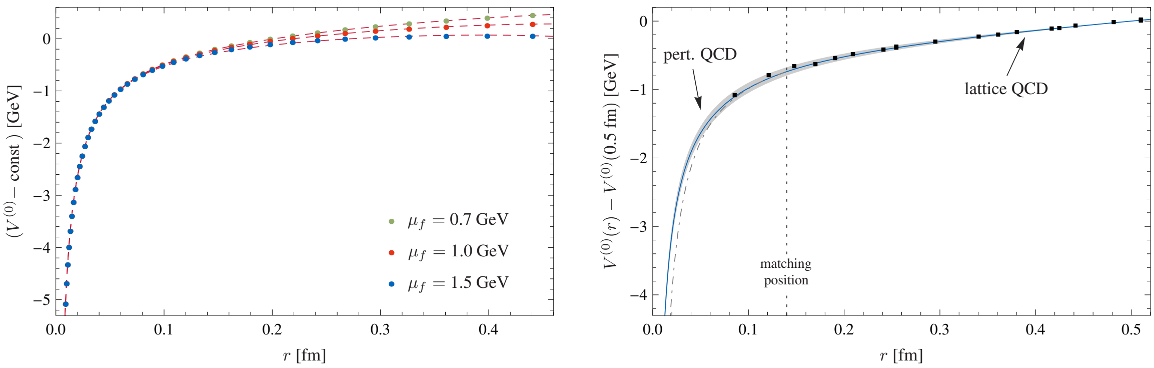

Figure 1: Static QCD potential (with $n_f = 3$) from the restricted numerical Fourier transform (6). Left: coordinate space potential at two-loop order for different values of μ_f. The curves have been shifted by a constant to match at small r values. Right: potential matched at $r = 0.14$ fm to a potential from lattice QCD [7]. Taken from Ref. [8].

where n_f is the number of light-quark flavors. Higher order terms have infrared contributions and are not considered at this level. Expressing $\alpha_s(|\vec{q}\,|)$ in a power series expansion about α_s at a fixed scale μ leads to the standard definition of the r-space static potential,

$$(5)\quad V^{(0)}(r) = -\frac{4}{3}\frac{\alpha_s(\mu)}{r}\left\{1 + \frac{\alpha_s(\mu)}{4\pi}\left[a_1 + 2\beta_0\, g_\mu(r)\right] + \left(\frac{\alpha_s(\mu)}{4\pi}\right)^2\left[a_2 + \beta_0^2\left(4g_\mu^2(r) + \pi^2/3\right) + 2g_\mu(r)(2a_1\beta_0 + \beta_1)\right] + \mathcal{O}(\alpha_s^3)\right\},$$

with $g_\mu(r) = \ln(\mu r) + \gamma_E$. It is well known that this potential suffers from renormalon ambiguities [4,5] and shows a badly convergent behavior [6].

We work in the following in the potential subtracted (PS) scheme proposed by Beneke [4] and define the static r-space potential,

$$(6)\quad V^{(0)}(r, \mu_f) = \int\limits_{|\vec{q}\,|>\mu_f} \frac{d^3q}{(2\pi)^3}\, e^{i\vec{q}\cdot\vec{r}}\, \tilde{V}^{(0)}(|\vec{q}\,|)\,,$$

where $\tilde{V}^{(0)}(|\vec{q}\,|)$ is given in Eq. (2), but $\alpha_s(|\vec{q}\,|)$ is understood without resorting to a power series expansion. The momentum space cutoff μ_f is introduced in order to exclude the uncontrolled low momentum region. The potential $V^{(0)}(r, \mu_f)$ is evaluated numerically using four-loop RGE running for the strong coupling α_s. For distances $r \lesssim 0.2$ fm, this potential depends only marginally on μ_f as shown in the left plot of Fig. 1. The perturbative potential, valid at small distances, can be matched at intermediate distances to results from lattice QCD (see the rightmost plot in Fig. 1). For the matching point (dashed line) we choose $r = 0.14$ fm where both the perturbative and lattice potential are expected to be reliable.

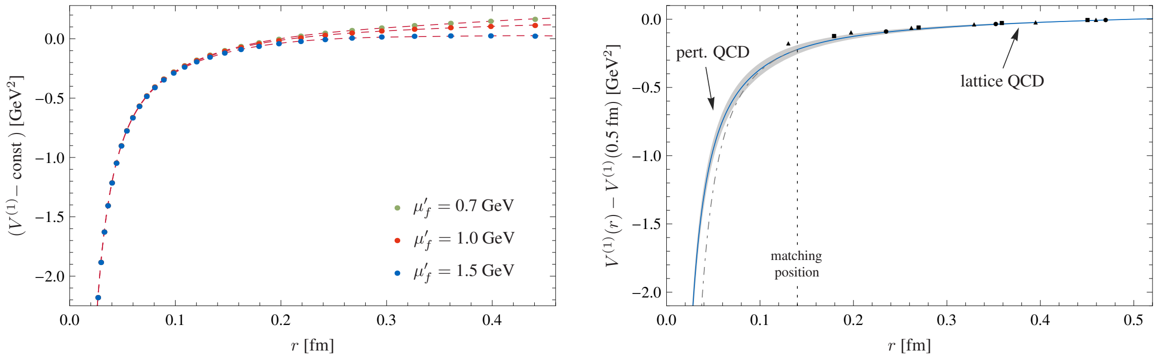

Figure 2: The order $1/m$ potential with $n_f = 3$, from the restricted Fourier transform. Left: perturbative potential for different cutoffs μ'_f. Right: perturbative potential matched at intermediate distances to a potential from lattice QCD. Taken from Ref. [8].

2 The order $1/\mathrm{m}$ potential and quarkonium spectroscopy

$V^{(1)}$ in Eq. (1) is the first mass dependent correction to the static potential. It is spin independent and the leading term reads in momentum space [9]:

$$\tilde{V}^{(1)}(|\vec{q}\,|) = -\frac{2\pi^2\alpha_s^2(|\vec{q}\,|)}{|\vec{q}\,|}\{1 + \mathcal{O}(\alpha_s)\}\,. \tag{7}$$

It can be transformed analogously as in Eq. (6) to r-space with a low momentum cutoff μ'_f. The dependence of $V^{(1)}$ on the cutoff scale is again very weak for distances $r \lesssim 0.2$ fm. At long distances $V^{(1)}(r)$ is known from lattice QCD [10, 11]. To fit the lattice data we use the form

$$V^{(1)}_{\text{fit}}(r) = -\frac{c'}{r^2} + d' \ln\left(\frac{r}{r_0}\right) + \text{const}, \tag{8}$$

motivated in [12]. As shown in Fig. 2 matching with the perturbative potential at intermediate distances is also possible at order $1/m$.

Using $V^{(0)}$ and $V^{(1)}$ as input in the Schrödinger equation, we can examine bottomonium and charmonium spectra. The overall constant of the potential is the only free parameter. This single parameter is related to the heavy quark mass in the PS scheme and can be translated in a second step to the bottom and charm quark masses in the $\overline{\text{MS}}$ scheme (see [8] for details). Our findings for the masses are summarized in Table 1 and compared to the values listed by the Particle Data Group (PDG) [13]. Results for the bottomonium and charmonium spectra are shown in Fig. 3. In both cases we find that the 1S states are the most strongly affected by $1/m$-effects. An additional effective one-gluon exchange spin dependent term with $\alpha_s^{\text{eff}} = 0.3$ (+h.f. in Fig. 3) would improve our predictions. Of course,

$\overline{\text{MS}}$ masses [GeV]			
	Static	Static + $\mathcal{O}(1/m)$	PDG 2010
Bottom quark	4.20 ± 0.04	$4.18^{+0.05}_{-0.04}$	$4.19^{+0.18}_{-0.06}$
Charm quark	1.23 ± 0.04	$1.28^{+0.07}_{-0.06}$	$1.27^{+0.07}_{-0.09}$

Table 1: Comparison of quark masses obtained in our approach (leading order plus order $1/m$ corrections) with the values listed by the Particle Data Group (PDG) [13].

this step is purely ad hoc and needs to be substituted by the full potential of order $1/m^2$, to be investigated in forthcoming work.

Acknowledgments

Work supported in part by BMBF, GSI and the DFG Excellence Cluster "Origin and Structure of the Universe".

References

[1] M. Peter, *Phys. Rev. Lett.* **78**, 602 (1997).

[2] M. Peter, *Nucl. Phys.* **B501**, 471 (1997).

[3] Y. Schröder, *Phys. Lett.* **B447**, 321 (1999).

[4] M. Beneke, *Phys. Lett.* **B434**, 115 (1998).

[5] A. H. Hoang, M. C. Smith, T. Stelzer, S. Willenbrock, *Phys. Rev.* **D59**, 114014 (1999).

[6] A. Pineda, *J. Phys.* **G29**, 371 (2003).

[7] G. S. Bali, et al., *Phys. Rev.* **D62**, 054503 (2000).

[8] A. Laschka, N. Kaiser, W. Weise, *Phys. Rev.* **D83**, 094002 (2011).

[9] N. Brambilla, A. Pineda, J. Soto, A. Vairo, *Phys. Rev.* **D63**, 014023 (2000).

[10] Y. Koma, M. Koma, H. Wittig, *Phys. Rev. Lett.* **97**, 122003 (2006).

[11] M. Koma, Y. Koma, H. Wittig, *PoS* **Confinement8**, 105 (2008).

[12] G. Perez-Nadal, J. Soto, *Phys. Rev.* **D79**, 114002 (2009).

[13] K. Nakamura, et al., *J. Phys.* **G37**, 075021 (2010).

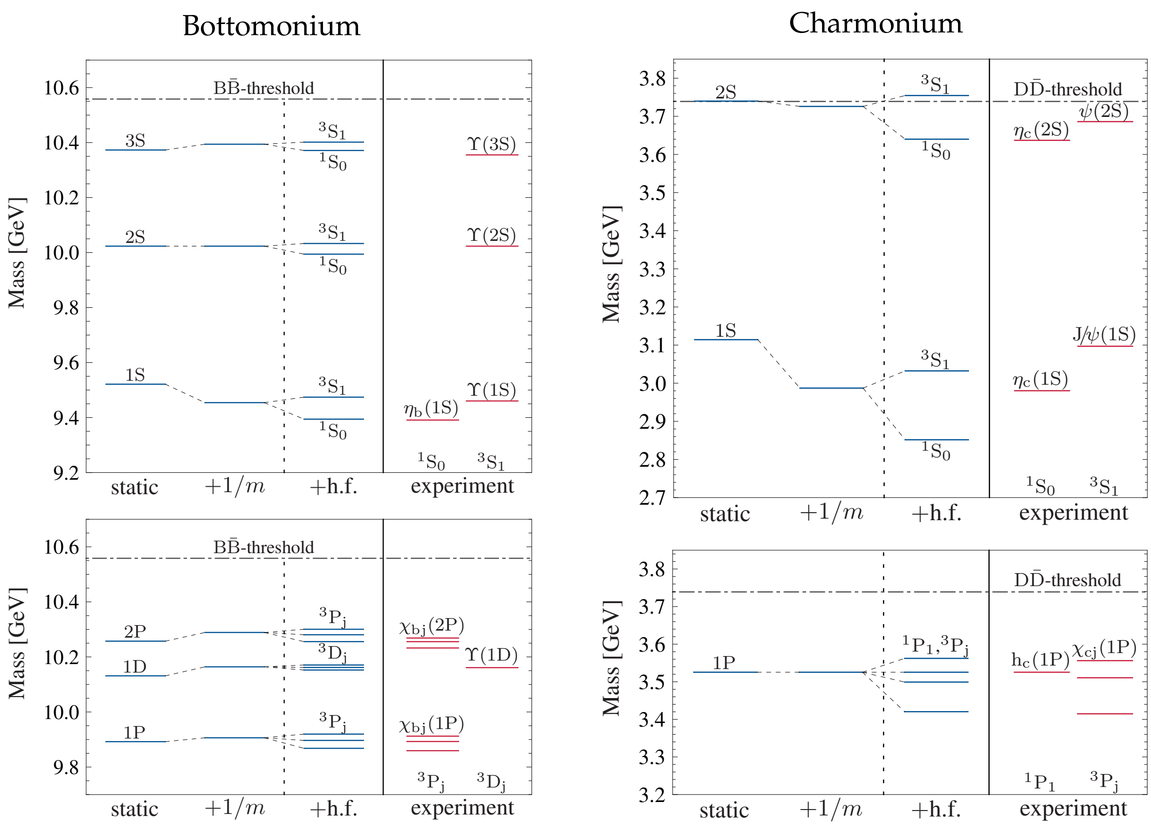

Figure 3: Bottomonium and charmonium spectrum in comparison with experiment. Static plus order $1/m$ results are shown, with additional hyperfine effects (h.f.) added phenomenologically. Taken from Ref. [8].